Study of the ANS Sympathovagal Behavior Using the ReliefF and the KS-Segmentation Algorithms

AHMED BOUZIANE[1,2], BENABDELLAH YAGOUBI[1], LUIS VERGARA[2], ADDISSON SALAZAR[2]
[1]Department of Electrical engineering
University of Mostaganem
P.O.Box 227 & 118, 27000 Mostaganem
ALGERIA
bouah@doctor.upv.es, yagoubibenabdellah@yahoo.com
[2]Institute of Telecommunications and Multimedia Applications
Universitat Politècnica de València
Camino de Vera, s/n 46022 Valencia
SPAIN
lvergara@dcom.upv.es, asalazar@dcom.upv.es

Abstract: - The Autonomous Nervous System (ANS) sympathovagal balance was studied using several features derived from Heart Rate Variability signals (HRV). The HRV signals are, however naturally, non-stationary since their statistical properties vary under time transition. A useful approach to quantifying them is, therefore, to consider them as consisting of some intervals that are themselves stationary. To obtain the latter, we have applied the so called the KS-segmentation algorithm which is an approach deduced from the Kolmogorov-Smirnov (KS) statistics. To determine, accurately, these features, we have used the ReliefF algorithm which is one of the most successful strategies in feature selection; this step allows us to select the most relevant features from thirty three features at the beginning. As result the ratio between LF and HF band powers of HRV signal, the Standard Deviation of RR intervals (SDNN), and Detrended Fluctuation Analysis with Short term slope (DFA α_1), are more accurate for each stationary segment, and present the best results comparing with other features for the classification of the three stages of stress in real world driving tasks (Low, Medium and High stress).

Key-Words: - HRV, KS-segmentation algorithm, Wavelet packet, ANS sympatho-vagal balance evolution

1 Introduction

It is well established by many studies that heartbeat can evaluate the autonomic nervous system (ANS) [1, 2, 3]. The latter has become increasingly popular because information on the behavior of the autonomic nervous system (ANS) can be noninvasively inferred using relatively simple signal processing methods [1]. A stress; emotional or mental, may lead to an increase in sympathetic activity and a decrease in parasympathetic activity of the ANS [4] which are, respectively, shown by energy concentration peaks in low frequency (0.04 to 0.15 Hz) and high frequency (0.15 to 0.4 Hz) ranges in the HRV power spectral density (PSD) curve [5]. This results in increased strain on the heart as well as on the immune and hormonal systems which influence the activity and balance of the autonomic nervous system (ANS). Many data, obtained in different experimental conditions involving human studies, have been gathered [6] to validate the following three main assumptions:

a) The respiratory rhythm of heart rate variability (HF) is a marker of vagal modulation.

b) The rhythm corresponding to vasomotor waves and present in heart rhythm and arterial pressure variability (LF) is a marker of sympathetic modulation of, respectively, heart rhythm and vasomotion, and c) The ratio LF/HF is a marker of the state of the sympathovagal balance modulating sinus node pacemaker activity [7,8,23].

To study this sympathovagal balance, Fourier transform is, usually, used in spectral analysis to compute the power spectral density (PSD) of the HRV [9, 10], but it does not depend on time; hence there is a lack of information such as the time when

the sympathetic or the parasympathetic activity is dominant, as well as how long this dominance lasts during the test period. This is, particularly, important when different events affecting the ANS are taking place and we need to link them to the (ANS) activities. The mathematical tools such as the short time Fourier transform (STFT) [16] or the wavelet transform that take into account both frequency and time are, therefore, welcomed.

In contrast to the STFT which is a time-frequency representation, the continuous wavelet transform method is a dynamical representation [11-15]. But there is, still, a correlation between the scale parameter and its corresponding frequency. Despite the useful results provided by these two methods [16, 17], difficulties, such as the scale range of the adequate continuous wavelet and the constant width of the STFT window, hampering their applications, are, however, met in each of them.

In this work, and based on our previous work [22, 24], we have used a hybrid method in order to classify the three stages of stress in real world driving tasks. Features were processed using the Relief algorithm [31] in small stationary segments which were determined and detected, accurately, using the KS-segmentation algorithm introduced recently by S. Camargo et al. [18].

2 Material and Method

2.1 Material and data collection

The data analyzed in this work were obtained from Stress Recognition in Automobile Drivers from PHYSIONET website [25], the driver database is originally collected by Healey & Picard from MIT Media Lab [26]. In total there are 17 available datasets, but according to Yong et.al [27], it was found that amongst the 17 data sets, only 7 drives datasets (drivers 6, 7, 8, 10, 11, 12, and 15) have clear mark identification and they can be used in our analysis.

This database contains a collection of multiparameter recordings from healthy volunteers, taken while they were driving on a prescribed route including city streets and highways in and around Boston, Massachusetts. The objective of the study for which these data were collected was to investigate the feasibility of automated recognition of stress on the basis of the recorded signals, which include ECG, EMG, GSR measured on the hand and foot, and respiration[25].

From the duration of different driving segment obtained from Table.1, it was validated that the rest, highway, and city driving periods produce the low, medium, and high levels of stress, respectively [26].

The driver database lacks the information regarding the duration of each Rest, City and Highway driving task, but the same durations were mentioned in [31]. The time intervals of the 7 drivers used in this study (drivers 6, 7, 8, 10, 11, 12, and 15) are given in Table.1.

In this study seven ECG records were used to test the algorithm. These recordings were sampled at 496 Hz with a 16-bit rate resolution. Lead II from each record is used here. No episodes have been excluded from our analysis.

Band pass filtering is an essential first stage of any QRS detection algorithm. The purpose of band pass filtering is to remove the baseline wander and high frequencies which do not contribute to QRS complexes detection. In this research, a band pass linear phase FIR digital filter with a Hamming window in the frequency range between 3 and 40 Hz is used [28].

Table.1. Time intervals of driving test.

Drive No	Driving period							Total rec. time (mn)
	Initiale Rest	City1	Highway1	City2	Highway2	City3	Final Rest	
Driver6	15.05	14.49	7.32	6.53	7.64	12.29	15.05	78.38
Driver7	15.04	16.23	10.96	9.83	7.64	10.15	15.03	84.87
Driver8	15	12.31	7.23	9.51	7.64	13.43	15.07	80.19
Driver10	15.04	15.3	8.66	5.27	7.04	12.06	14.79	78.15
Driver11	15.02	15.81	7.43	7.15	6.96	11.72	14.99	79.08
Driver12	15.01	13.41	7.56	6.5	8.06	11.68	15.01	77.23
Driver15	15	12.54	7.24	5.99	6.82	12.12	15	74.7

The extraction of R-peaks and correction of artifacts from digitized ECG data were performed using ARTiiFACT [29], which is a software tool providing an efficient artifact detection algorithm.

All extracted features of HRV signals were calculated using the Kubios HRV Analysis 2.0 software [30]. The program calculates all the commonly used time and frequency domain parameters and the nonlinear Poincare plot. Advanced spectrum estimation methods and detrendingoptions are included as well. All records were processed using MATLAB (R2012a 7.14.0.739).

2.2 Hybrid method for studying the ANS activity

The suggested hybrid method to classify stress in order to study the ANS balance can be described by the following steps:

1-The ECG signal is preprocessed using band-pass filter; later ARTiiFACT tool is used on filtered ECG signal to enhance the presence of QRS complexes and to detect R-Peaks and finally the HRV signals are calculated.
2-Segment each HRV signals into stationary patches by applying the KS-segmentation algorithm.
3-Compute 33 features in each stationary segment of the temporal signals using Kubios HRV Analysis Software. Table.2 presents a detailed description of all features.
4- The next step is to calculate and extract the most relevant features; we have used the ReliefF algorithm, this algorithm try to find features that help separate data of different classes. If a feature has no effect on class-based separation, it can be removed.

These main steps of this suggested hybrid method are depicted in the following diagram in Fig.1.

Table.2. Description of the 33 extracted features.

	Features	Units	Description
Time Domain	Mean RR	[ms]	The mean of RR intervals
	STD RR (SDNN)	[ms]	Standard deviation of RR intervals
	Mean HR	[1/min]	The mean heart rate
	STD HR	[1/min]	Standard deviation of intantaneous HR values
	RMSSD	[ms]	Square root of the mean squared differences between successive RR intervals
	NN50		Number of successive RR interval pairs that differ more than 50 ms
	pNN50	[%]	NN50 divided by the total number of RR intervals
	HRV triangular index		The integral of the RR interval histogram Divided by the height of the histogram
	TINN	[ms]	Baseline width of the RR interval histogram
Frequency Domain	Peak frequency	[Hz]	VLF, LF, and HF band peak frequencies
	Absolute power	[ms^2]	Absolute powers of VLF, LF, and HF bands
	Relative power	[%]	Relative powers of VLF, LF, and HF bands
	Normalized power	[n.u.]	Powers of LF and HF bands in normalized units
	LF/HF		Ratio between LF and HF band powers
Nonlinear	SD1, SD2	[ms]	The standard deviation of the Poincare plot perpendicular to (SD1) and along (SD2) th line-of-identity
	ApEn		Approximate entropy
	SampEn		Sample entropy
	D_2		Correlation dimension
	DFA α_1		Detrended fluctuation analysis with Short term slope
	DFA α_2		Detrended fluctuation analysis with Long term slope
	RPA Lmean	[beats]	Recurrence plot analysis of Mean line length
	RPA Lmax	[beats]	Recurrence plot analysis of Maximum line length
	RPA REC	[%]	Recurrence plot analysis of Recurrence rate
	RPA DET	[%]	Recurrence plot analysis of Determinism
	RPA ShanEn		Recurrence plot analysis of Shannon entropy

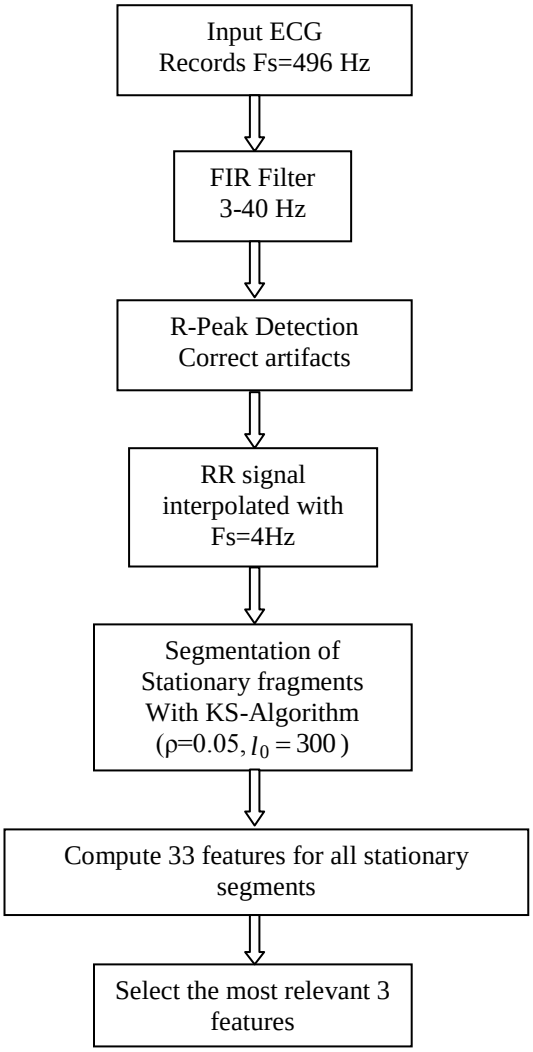

Fig.1 The flow chart of the proposed hybrid method.

3 Results and Discussion

The aim of a heart rhythm representation is to provide a signal that should accurately reflect variations in the heart rhythm behavior, and which should lend itself to much kind of processing. An example of such HRV variation in time is depicted in Fig.2. The heart rhythm is, usually, represented in terms of rate which is given by the inverse of the RR inter beat intervals. The variation of this inverse in time, represents, thus, the HRV signal.

The goal of our method, to study the ANS, is to use features from HRV signals to detect stress of automobile driver's, HRV analysis is commonly used as a quantitative marker depicting the activity of ANS that may be related to mental stress [32].

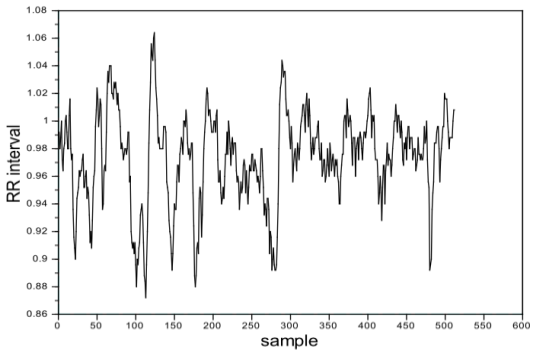

Fig.2 Cardiac interbeat (RR) interval time series.

The RR interval signal is usually interpolated to recover an evenly sampled signal. Cubic interpolation is adopted and the resampling frequency of the interpolated signal is Fs=4Hz [21]. As mentioned above in the introduction, the sympathetic and the parasympathetic activities of the ANS are empirically situated in low frequency (LF) and high frequency (HF) ranges, respectively in the Fourier space [22]. When these activities are taking place, the HRV power spectral density curve shows large concentration of energy in these frequency ranges, and the sympathovagal balance is, usually, estimated using the PSD in the LF to that in the HF ratio (LF/HF). So, in addition of this PSD ratio, we have computed 32 other features to track the evolution of the ANS behavior as well as the localization in time of its activities.

In order to compute, accurately, this features, first, we have to segment these HRV signals into stationary segments, since any signal is thought of as being composed of small stationary segments. To identify accurately the latter, many algorithms, such as those based on Student's t statistic [29], have been proposed, but they present some difficulties in determining, accurately, the stationary segments. S. Camargo et al [18] have, recently, introduced an algorithm named K-S segmentation algorithm to determine more accurately the stationary segments for a given signal using an approach based on Kolmogorov-Smirnov (KS) statistic. It should be noted that the KS-segmentation algorithm which is described in (Fig.3) is different from the KS statistic. More details about this segmentation algorithm can be found in S Camargo et al work [18].

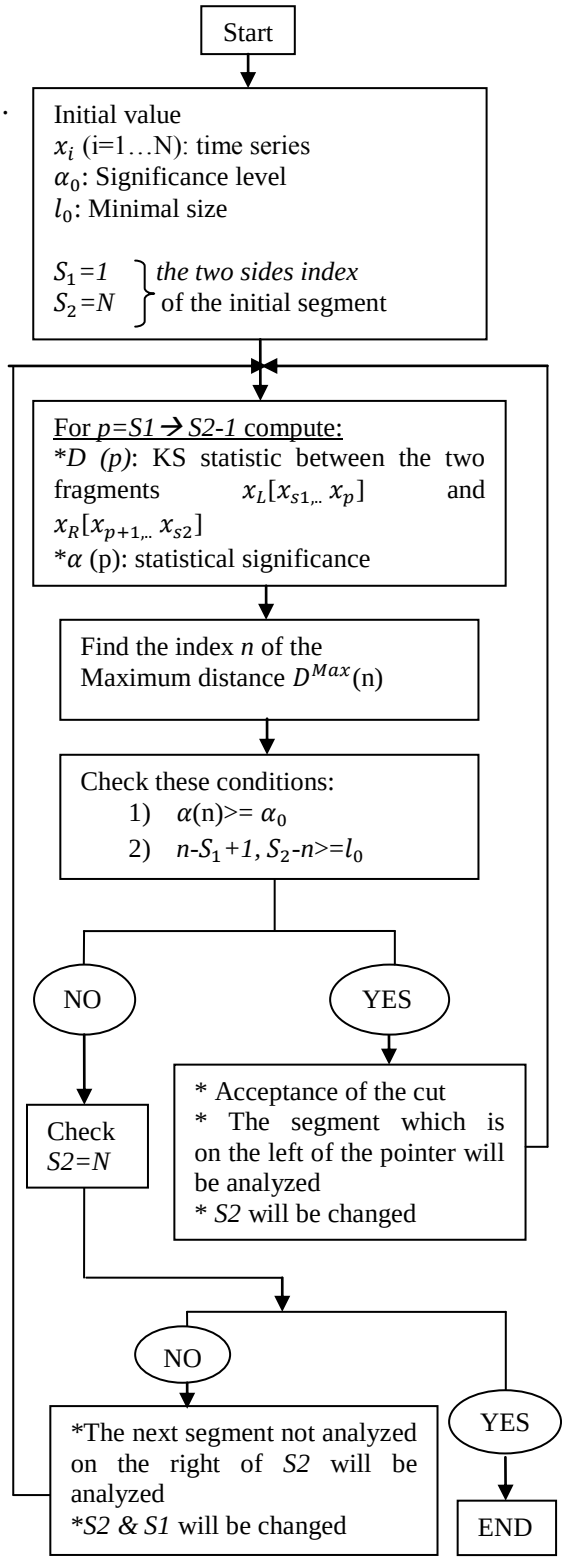

Fig.3 The KS-Segmentation algorithm

To obtain a more accurate segmentation of the HRV temporal signals into stationary patches, we have chosen to work with:

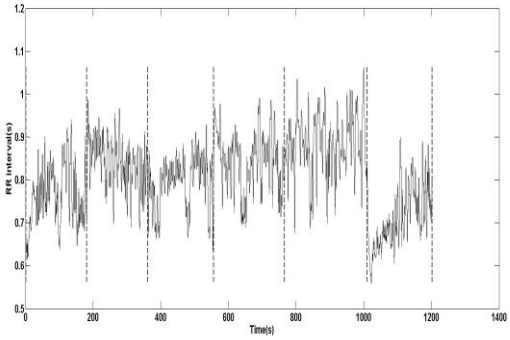

Fig.4 Part from temporal HRV signal for driver06, the stationary segments obtained using the KS-segmentation algorithm are delimited by the vertical lines.

-A minimal stationary segment length or number of points $L_0 = 720$ (3mn), to distinguish between the three main spectral components [1], (as a result, the lowest frequency that can be resolved is 1/180≈0.0055Hz, just above the lower limit of the VLF region).

-A statistical significance level $P_0 = 0.99$ considered as an acceptable and standard level for this kind of distribution test [18], is illustrated in (Fig.4) for the Driver 06 as an example. The vertical discontinuous lines shown in this figure delimit these stationary segments obtained by the KS-segmentation algorithm.

Once these stationary patches have been obtained, all features will be computed using Kubios HRV Analysis Software, for each stationary segment *i* of the HRV signals.

For thre feature selection ReliefF algorithm is context sensitive, robust, and can deal with datasets with highly interdependent features, with incomplete and noisy data and can be used for evaluating the feature quality in multi-class problems. Instead of *n* nearest hits and misses, ReliefF searches for n nearest instances from each class. The contributions of different classes are weighted with their prior probabilities. For a more thorough overview of feature quality measures, see [31]. The description of the Algorithm is provided in the Fig.5. Initial values are:

-*M* learning instances x_k (*N* features and *C* classes);

-Probabilities of classes p_y; Sampling parameter *m*;

-Number *n* of nearest instances from each class;

```
1  for i = 1 to N do W[i] = 0.0; end for;
2  for l = 1 to m do
3    randomly pick an instance x_k (with class y_k);
4    for y = 1 to C do
5      find n nearest instances x[j, y] from class y, j = 1..n;
6      for i = 1 to N do  for j = 1 to n do
7        if y = y_k { nearest hit? }
8          then W[i] = W[i] – diff(i,x_k,x[j, y])/(m * n);
9          else W[i] = W[i] + p_y/(1 − p_{y_k})* diff(i,x_k,x[j, y])/(m * n);
10       end if;
11     end for; { j }  end for; { i }
12   end for; { y }
13 end for; { l }
14 return(W);
```

Fig.8 ReliefF Algorithm.

For output value, each feature F_i a quality weight $-1 \leq W[i] \leq 1$;

Quality estimations W can also be negative, however, W $[F_i] \leq 0$ means that feature F_i is irrelevant.

We have divided the whole driving time into 7 periods according to the Table.1, with respect to different stress class values drivers, each period has at least one stationary segments.

These 33 features were used to create a single vector representing each of the segments used in the feature analysis. A total of 83 segments were extracted from the 7 drivers: 28 from rest periods, 27 from highway driving, and 28 from city driving. The resulting 83 feature vectors were then used with target values taken from Table.1, for the selection of the best relevant features.

We have calculated the weights of 33 features for all 7 drivers, and to get a good idea we have calculated the sum of the weights for all features. To better observe the values we have multiplied all the values by 100, so this is a percentage ($-100 \leq W[i] \leq 100$). All results are shown in Table.3, Table.4, and Table.5.

Table.3 The percentage of feature weights in Time Domain

Features	Driver6	Driver7	Driver8	Driver10	Driver11	Driver12	Driver15	Total
Mean RR	5,4265141	0,94608789	2,15877276	-0,3673764	7,08424454	2,06492077	3,82870738	21,141871
STD RR (SDNN)	-1,12031473	5,30112026	3,64183896	12,4138418	1,41023324	1,36558239	6,36862085	29,3809227
Mean HR	5,04576079	1,48723939	2,18555675	-0,1654806	7,43518712	5,80068335	4,02173856	25,8106854
STD HR	0,64459831	4,03596799	3,00599826	5,48175498	0,99390922	2,48964014	7,08112023	23,7329891
RMSSD	4,43330983	5,27276105	4,63776719	3,60629526	2,4912859	1,3390948	-0,6543828	21,1261312
NN50	4,93499129	3,75716757	5,89490642	4,09302749	2,42414003	-1,1514342	-1,1191262	18,8336723
pNN50	4,1131347	5,2578275	5,70706436	-2,49139871	7,06734887	-2,09602672	1,00740149	18,5653515
HRV triangular index	3,98374543	8,66282	1,17147445	3,79857956	2,9558076	2,54509804	4,03950875	27,1570338
TINN	-0,50005994	3,94967263	2,98269825	7,31407287	3,10674207	3,03159291	5,41442861	25,2991474

Table.4 The percentage of feature weights in Frequency Domain

Features	Driver6	Driver7	Driver8	Driver10	Driver11	Driver12	Driver15	Total
Peak VLF	-1,870995	-0,240218	-0,501896	-4,6579505	-1,4490866	5,25749220	-1,97545442	-5,438110603
Peak LF	-1,455172	3,2278905	-0,101692	-6,6279138	-0,8270396	6,11780911	0,33046205	0,664342529
Peak HF	9,7373692	2,8587799	1,250429	27,686010	2,0393704	1,55724029	-2,43878988	42,69041027
Absolute power VLF	-0,043268	1,8839376	3,3143432	-2,4180459	2,6976153	-1,4494387	7,43173916	11,41688249
Absolute power LF	0,6045780	4,7026317	2,6913606	12,1786356	1,6473066	-2,2639601	0,15869727	19,71924984
Absolute power HF	5,9716729	2,9236121	6,7313311	5,95757061	6,68760858	-1,2680803	1,55811979	28,56183483
Relative power VLF	4,0004530	3,4704776	5,1832699	-5,7655098	3,8176044	-2,3362531	3,41283561	11,78287771
Relative power LF	1,3066848	4,5676953	0,8556610	3,5804381	-0,0989818	-0,3357334	0,92373378	10,79949792
Relative power HF	4,3671313	-3,404726	6,4272542	7,72285027	5,6769006	5,29946549	6,28937362	32,37824898
Normalized power LF	1,6750151	2,7055632	3,7379327	9,11338152	4,34139307	14,0069736	3,75061345	39,33087282
Normalized power HF	2,1862527	1,8313037	5,2671011	11,3037182	5,53590517	7,75041689	7,03267480	40,90737281
LF/HF	2,1862527	1,8313037	5,2745638	11,3037182	5,53590517	7,75041689	7,03267480	40,91483546

Table.5 The percentage of feature weights in Nonlinear measures

Features	Driver6	Driver7	Driver8	Driver10	Driver11	Driver12	Driver15	Total
SD1	4,481071723	5,265676992	4,625379042	3,590119996	5,908918707	1,270657762	-0,63200023	24,50982399
SD2	-0,89913093	5,155896285	3,949342831	12,30070408	1,299309636	1,740719033	6,916938265	30,4637792
RPA Lmean	1,130658558	1,487489835	1,559821106	-5,17918950	1,18132893	5,403955316	0,010057975	5,594122218
RPA Lmax	1,897946925	1,75672714	4,240080664	-2,51557777	2,330251115	7,531546255	2,820652947	18,06162727
RPA REC	5,285340028	2,39446695	2,990843723	-4,00252028	2,33608176	3,493944552	4,860862169	17,3590189
RPA DET	8,336087485	2,357117419	1,297534119	2,076421438	3,749714864	2,896763256	6,060281398	26,77391998
RPA ShanEn	4,45967594	1,406204097	0,885551438	-2,86795753	2,450600875	4,312108289	2,26727989	12,913463
ApEn	2,65257873	4,343730032	4,2239E-16	-7,35371131	1,078834562	8,666119087	1,96788185	11,35543294
SampEn	3,302008024	4,215304831	0,489753063	4,950714233	2,078023777	4,666590115	-1,21892079	18,48347325
DFA α1	2,596206618	1,329679378	4,468054587	10,33841569	6,569025917	0,610299735	7,625394253	33,53707618
DFA α2	4,827956397	6,17605819	3,694075334	-7,99819723	2,255482084	-2,11124932	5,513654621	12,35778007
D2	6,301947561	-0,91726545	0,283827833	-6,39944059	-1,81097229	6,043045703	0,313220789	3,814363548

Comparing between all the results In these three tables we can see that there are some features are relevant and we can easily see the difference, in the time domain features Standard deviation of RR intervals present the most relevant feature for the distinction between the three stress stages, following by The integral of the RR interval histogram divided by the height of the histogram (HRV triangular index).

In the Frequency domain there are 4 relevant features can be used in stress detection, they are: Ratio between LF and HF band powers, Powers of LF and HF bands in normalized units and HF band peak frequencies.

In Nonlinear measures it is obvious that Detrended fluctuation analysis with Short term slope present the best choice to classify stress in similar situations.

4 Conclusion

The suggested hybrid method based on the KS-segmentation algorithm, to determine the stationary segments, as well as the application of the ReliefF algorithm for the feature selection to study the HRV evolution in time, seems to be simple, more accurate and easy to implement. According to our results using the proposed hybrid method, it is possible to confine the correlation between the LF/HF ratio and sympathovagal balance during stress period. Also we can propose in feature work study in more details relation between stress and some nonlinear measures as for example Detrended fluctuation with Short term slope for the good results obtained. This study may help in linking the ANS behavior to the corresponding stress situation.

Acknowledgements: The authors are very grateful to the European Commission presented by the EMMAG program, for the support of this work.

References:

[1] Task Force of the European Society of Cardiology and the North American Society of Pacing and Electrophysiology, Heart Rate Variability: Standards of Measurement, Physiological Interpretation, and Clinical Use, *Circulation*, Vol.93, No.5, 1996, pp.1043–1065.

[2] Kohara K, Nishida W, Maguchi M, Hiwada K, Autonomic Nervous Function in Non-Dipper Essential Hypertensive Subjects: Evaluation by Power Spectral Analysis of Heart Rate Variability, *Hypertension*, Vol.26, No.5, 1995, pp.808–814.

[3] Winchell RJ, Hoyt DB, Spectral Analysis of Heart Rate Variability in the Icu: A Measure of Autonomic Function, *Journal of Surgical Research*, Vol.63, No.1, 1996, pp.11–16.

[4] Raquel Bailón, Luca Mainardi, Michele Orini, Leif Sörnmo, Pablo Laguna, Analysis of Heart Rate Variability During Exercise Stress Testing Using Respiratory Information, *Biomedical Signal Processing and Control*, Vol.5, No.4, 2010, pp.299–310.

[5] M. Malik and A. J. Camm, *Heart Rate Variability*, Futura Publishing, 1995

[6] Malliani, A., M. Pagani, F. Lombardi, and S. Cerutti, Cardiovascular Neural Regulation Explored in the Frequency Domain, *Circulation*, Vol.84, No.2, 1991, pp.482–492.

[7] N Montano, T G Ruscone, A Porta, F Lombardi, M Pagani and A Malliani, Power Spectrum Analysis of Heart Rate Variability to Assess the Changes in Sympathovagal Balance During Graded Orthostatic Tilt, *Circulation*, Vol.90, No.4, 1994, pp.1826–1831.

[8] M. Bootsma, C. A. Swenne, H. H. Van Bolhuis, P. C. Chang, V. M. Cats, and A. V. Bruschke, Heart Rate and Heart Rate Variability as Indexes of Sympathovagal Balance, *Am J Physiol Heart Circ Physiol*, Vol.266, No.4, 1994, pp. H1565– H1571.

[9] Kay SM, Marple SL, Spectrum Analysis: A Modern Perspective, *Proc IEEE*, Vol.69, No.11, 1981, pp.1380–1419.

[10] Juan Sztajzel, Heart Rate Variability: A Noninvasive Electrocardiographic Method to Measure the Autonomic Nervous System, *Swiss Medical Weekly*, Vol.134, No.35, 2004, pp.514–522.

[11] U. Wklund, M. Akay and U. Niklasson, Short-Term Analysis of Heart-Rate Variability by Adapted Wavelet Transforms, *IEEE Eng. Med. Biol*, Vol.16, No.5, 1997, pp.113–138.

[12] Y. Meyer, *Les Ondelettes, Algorithmes, et Applications*, Armand Colin, 1992.

[13] I. Daubechies, *Ten Lectures on Wavelets*, SIAM, 1992.

[14] G. Strang and T. Nguyen, *Wavelets and Filter Banks*, Wellesley-Cambridge Press, 1996.

[15] R. Kronland-Martinet, J. Morlet and A. Grossmann, Analysis of Sound Patterns Through Wavlet Transforms, *Int.J Pat Recogn. Artif. Intel*, Vol.1, No.2, 1987, pp.97–126.

[16] S. Elsenbruch, Z. Wang, W. C. Orr, and D. Z. Chen, Time-Frequency Analysis of Heart Rate Variability Using Short-Time Fourier Transform, *Physiol Meas*, Vol.21, No.2, 2000, pp.229–240.

[17] M. Akay, Introduction:Wavelet Transforms in Biomedical Engineering, *Annals of Biomedical Engineering*, Vol.23, No.5, 1995, pp.529–530.

[18] S. Camargo, S. M. Duarte Quieros and C. Anteneodo, Nonparametric Segmentation of Nonstationary Time Series, *Physical Review E*, Vol.84, 2011, 046702.

[19] Bernaola-Galvan, P. Ch. Ivanov, L. A. N. Amaral, and H. E. Stanley, Scale Invariance in the Nonstationarity of Human Heart Rate, *Phys. Rev. Lett*, Vol.87, 2001, 168105.

[20] Alberto Malliani, The Pattern of Sympathovagal Balance Explored in the Frequency Domain, *Physiology*, Vol.14, No.3, 1999, pp.111–117.

[21] Bernaola-Galvan, P. Ch. Ivanov, L. A. N. Amaral, and H. E. Stanley, Scale Invariance in the Non-stationarity of Human Heart Rate, *Phys. Rev. Lett*, Vol.87, 2001, 168105.

[22] A.Bouziane, B.Yagoubi, L.Vergara, A.Salazar, The ANS Sympathovagal Balance Using a Hybrid Method Based on the Wavelet Packet and the KS-Segmentation Algorithm, *Advances in Circuits, Systems, Signal Processing and Telecommunications*, 2015, pp.75-83.

[23] S. SEYEDTABAII, Analysis of Heart Rate Variation Filtering Using LMS Based Adaptive Systems, *WSEAS TRANSACTIONS on SIGNAL PROCESSING*, Vol.04, No.04, 2008, pp.241–250.

[24] A.Bouziane, B.YagoubiAnd, S.Benkraouda, Method for Estimating the Duration of the ANS Sympathetic and Parasympathetic Activities, *Advances in Electrical and Computer Engineering*, 2015, pp.178-182.

[25] http://www.physionet.org/physiobank/database/drivedb/

[26] Healey JA, Picard RW, Detecting stress during real-world driving tasks using physiological sensors, *IEEE Transactions in Intelligent Transportation Systems*, Vol.06, No.2, 2005, pp.156–166.

[27] Deng Y, Wu Z, Chu CH, Zhang Q, Hsu DF, Sensor feature selection and combination for stress identification using combinatorial fusion, *Int J Adv Rob Syst*, Vol.10, No.3, 2013, pp.1–10.

[28] Ahambi, J. S., Tandon, S. N., Bhatt, R. K. P, Using wavelet transforms for ECG characterization. An on-line digital signal processing system, *Engineering in Medicine and Biology Magazine, IEEE*, Vol.16, No.1, 1997, pp.77–83.

[29] Kaufmann, T., Sütterlin, S., Schulz, S.M., Vögele, ARTiiFACT: a tool for heart rate artifact processing and heart rate variability analysis, *Behavior Research Methods*, Vol.43, No.4, 2011, pp.1161–1170.

[30] Niskanen, J.-P., Tarvainen, M.P., Ranta-Aho, P.O., Karjalainen, P.A., Software for advanced HRV analysis, *Computer Methods and Programs in Biomedicine*, Vol.76, No.1, 2004, pp.73–81.

[31] Huan Liu and Hiroshi Motoda, *Computational Methods of Feature Selection*, Chapman and Hall/CRC Press, 2008.

[32] L. Salahuddin and D. Kim, Detection of Acute Stress by Heart Rate Variability Using a Prototype Mobile ECG Sensor, *International Conference on Hybrid Information Technology*, Vol.2, 2006, pp.453–459.